

Supporting Information

**Concentration-Dependent Structural Transition of the HIV-1 gp41  
MPER Peptide into  $\alpha$ -Helical Trimers**

*Sai Chaitanya Chiliveri, John M. Louis, and Ad Bax\**

anie\_202008804\_sm\_miscellaneous\_information.pdf

## Table of Contents

Table of Contents .....	1
Experimental Procedures .....	1
Figure S1 .....	3
Figure S2 .....	4
Figure S3 .....	5
Figure S4 .....	6
Figure S5 .....	7
Figure S6 .....	8
Figure S7 .....	9
Figure S8 .....	10
Figure S9 .....	11
Figure S10 .....	12
Figure S11 .....	13
Author Contributions .....	15

## Experimental Procedures

### Sample preparation

Peptides MPER (Ac-GLLELNKWASLWNWFNKKKKK), MPER<sup>ΔN</sup> (Ac-GELNKWASLWNWFNKKKKK), MPER<sup>D664</sup> (Ac-GLLELDKWASLWNWFNKKKKK) and MPER<sup>trunc</sup> (Ac-GELNKWASLWN) were chemically synthesized, purified by reverse phase HPLC, and characterized by mass spectroscopy. All peptides were acetylated at their N-terminus.

### NMR chemical shift assignments

<sup>1</sup>H-<sup>13</sup>C HSQC spectra of samples in 95% H<sub>2</sub>O, 5% D<sub>2</sub>O were collected on Bruker Avance 700-MHz or 800-MHz NMR spectrometers, both equipped with a x, y, z-gradient cryogenic probe. <sup>1</sup>H-<sup>13</sup>C HSQC spectra in D<sub>2</sub>O and <sup>1</sup>H-<sup>15</sup>N HSQC spectra in H<sub>2</sub>O were collected on a Bruker Avance 600-MHz spectrometer, equipped with a z-gradient cryogenic probe. Two-dimensional TOCSY (mixing time τ<sub>m</sub> = 80 ms), NOESY (mixing time τ<sub>m</sub> = 200 ms), and ROESY spectra (mixing time τ<sub>m</sub> = 100 ms; 7 kHz spin lock field) were acquired at 800 MHz. NMR data were processed and analyzed using NMRPipe software<sup>[1]</sup> and figures were generated using nmrglue.<sup>[2]</sup>

### Data fitting

Concentration titration series were fit using standard monomer-dimer and monomer-trimer models. The following equations were used for this analysis.

#### Monomer-dimer association model:



$$K_d = \frac{[M]^2}{[D]} \quad (2)$$

$$[M_{tot}] = [M] + 2 \frac{[M]^2}{K_d} \quad (3)$$

$$[M] = \frac{-K_d + \sqrt{K_d^2 + 8K_d[M_{tot}]}}{4} \quad (4)$$

$$\delta = (\delta_{mon} * f_{mon}) + (\delta_{dim} * f_{dim}) \quad (5)$$

$$f_{mon} + f_{dim} = 1 \quad (6)$$

where δ is the chemical shift at a particular fraction of monomer (f<sub>mon</sub>) and dimer (f<sub>dim</sub>). δ<sub>mon</sub> and δ<sub>dim</sub> are the absolute chemical shifts of monomer and dimer, respectively. [M] and [D] are the concentrations of monomer and dimer, whereas [M]<sub>tot</sub> is the total concentration

## SUPPORTING INFORMATION

of the peptide. The least squares fitting was performed on chemical shifts obtained from a series of spectra recorded at different sample concentrations, using equations (4) and (5) to estimate the coefficient of dissociation,  $K_d$ . The coefficient of association is given by  $K_a = (1/K_d)$ .

**Monomer-trimer association model:**

$$K_d = \frac{[M]^3}{[T]} \quad (8)$$

$$[M_{tot}] = [M] + 3 \frac{[M]^3}{K_d} \quad (9)$$

$$[M] = \frac{1}{3} \left\{ \frac{\sqrt[3]{\sqrt{4K_d^3 + 81K_d^2[M_{tot}]^2 + 9K_d[M_{tot}]} + 3\sqrt[3]{2}K_d}}{\sqrt[3]{2}} - \frac{\sqrt[3]{\sqrt{4K_d^3 + 81K_d^2[M_{tot}]^2 + 9K_d[M_{tot}]} + 3\sqrt[3]{2}K_d}}{\sqrt[3]{\sqrt{4K_d^3 + 81K_d^2[M_{tot}]^2 + 9K_d[M_{tot}]}}} \right\} \quad (10)$$

$$\delta = (\delta_{mon} * f_{mon}) + (\delta_{tri} * f_{tri}) \quad (11)$$

$$f_{mon} + f_{tri} = 1 \quad (12)$$

where  $\delta$  is the chemical shift at a particular fraction of monomer ( $f_{mon}$ ) and trimer ( $f_{tri}$ ).  $\delta_{mon}$  and  $\delta_{tri}$  are the chemical shifts of monomer and trimer, respectively.  $[M]$  and  $[T]$  are the concentrations of monomer and trimer, whereas  $[M]_{tot}$  is the total concentration of the peptide. The least squares fitting was performed on chemical shifts obtained for a series of concentrations, using equations (10) and (11), to derive the dissociation coefficient,  $K_d$ .

**Thermodynamic properties**

The free energy of the association of three monomers into a trimer was calculated as,

$$\Delta G = -RT \ln(K_a) \quad (13)$$

The thermodynamic properties,  $\Delta H$ ,  $\Delta S$  were derived from the temperature dependence of  $K_a$  by using

$$\ln(K_a) = -\frac{\Delta H}{RT} + \frac{\Delta S}{R} \quad (14)$$

where  $R$  is the gas constant ( $0.00198 \text{ kcal K}^{-1} \text{ mol}^{-1}$ ).

**Circular Dichroism**

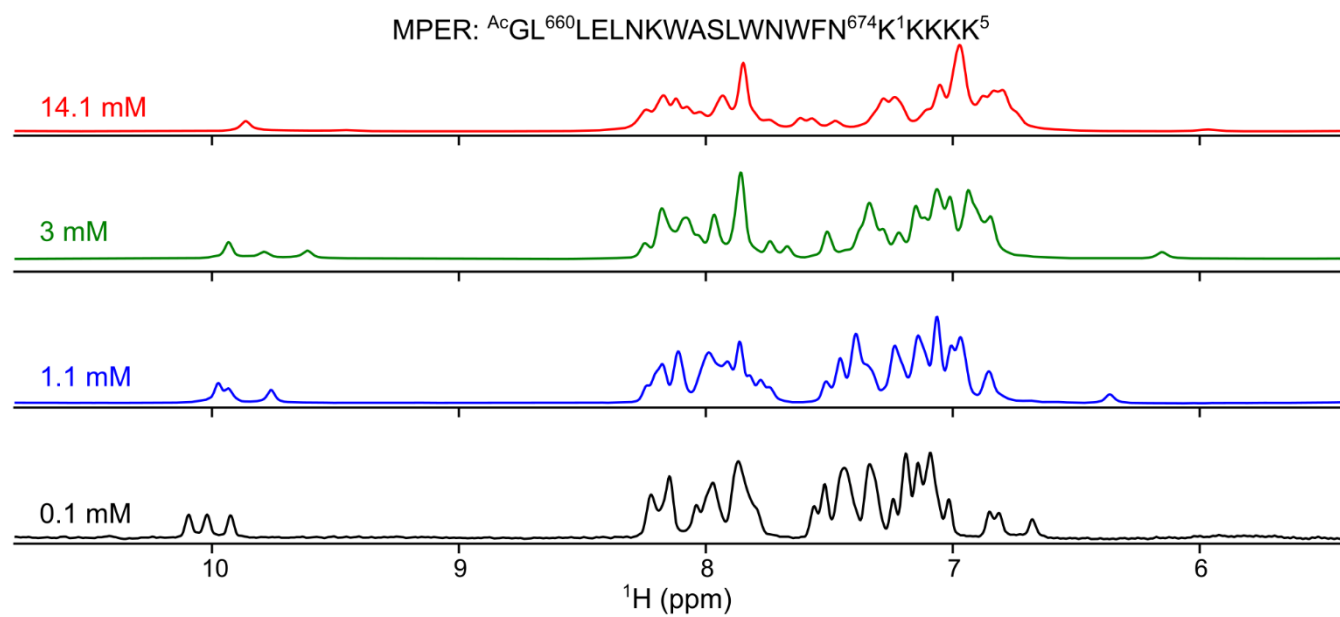
CD spectra were acquired in 20 mM sodium phosphate buffer (pH 6) and 50 mM NaCl on a JASCO J-810 spectropolarimeter at 25 °C. Data on low (0.025, 0.05 and 0.1 mM), intermediate (0.22, 0.34, and 0.68 mM) and high (3.4 and 6.8 mM) concentrations of MPER were collected using 0.1, 0.01 and 0.001 cm pathlength cuvettes, respectively. CD spectra of the single chain 6-helix bundle (6HB)<sup>[3]</sup> were acquired using 0.1 (5  $\mu\text{M}$ ), 0.01 (50  $\mu\text{M}$ ), and 0.001 (208 and 415  $\mu\text{M}$ ) cm pathlength cuvettes in 20 mM sodium formate (pH 4) buffer.

**Hydrogen Exchange**

HX rates were measured at 800-MHz  $^1\text{H}$  frequency, 35 °C on samples containing 0.25 mM and 4.3 mM MPER in 95%  $\text{H}_2\text{O}$ , 5%  $\text{D}_2\text{O}$ , 10 mM Imidazole buffer, pH 6.2. Rates were measured using the WEX-III scheme<sup>[4]</sup> adapted to analyze the intensities of amide ( $F_1$ ) to aliphatic ( $F_2$ ) cross peaks in 2D-TOCSY ( $\tau_m = 80 \text{ ms}$ ) spectra, with the pulse sequence preceded by six delay durations for the water inversion interval, ranging from 5 ms to 1 s (Figure S6).

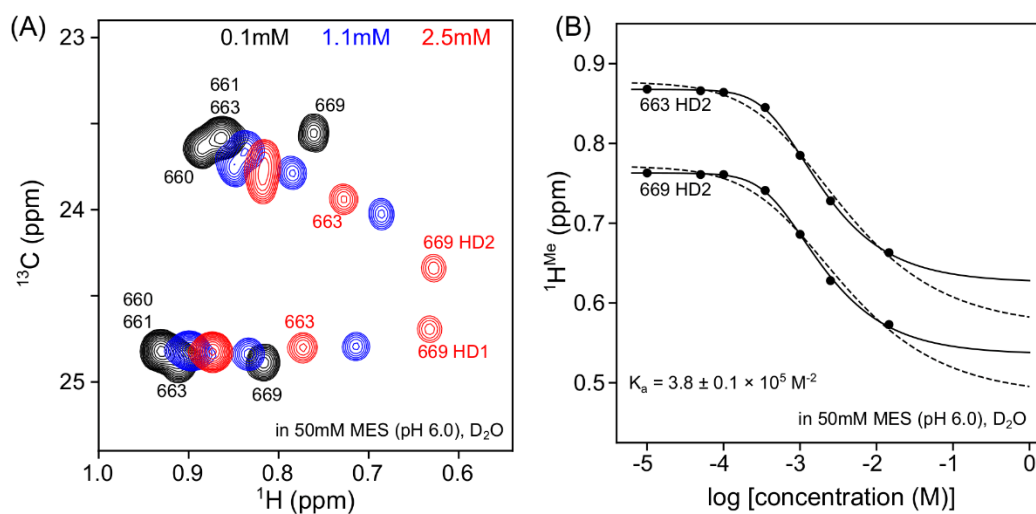
## SUPPORTING INFORMATION

Figure S1



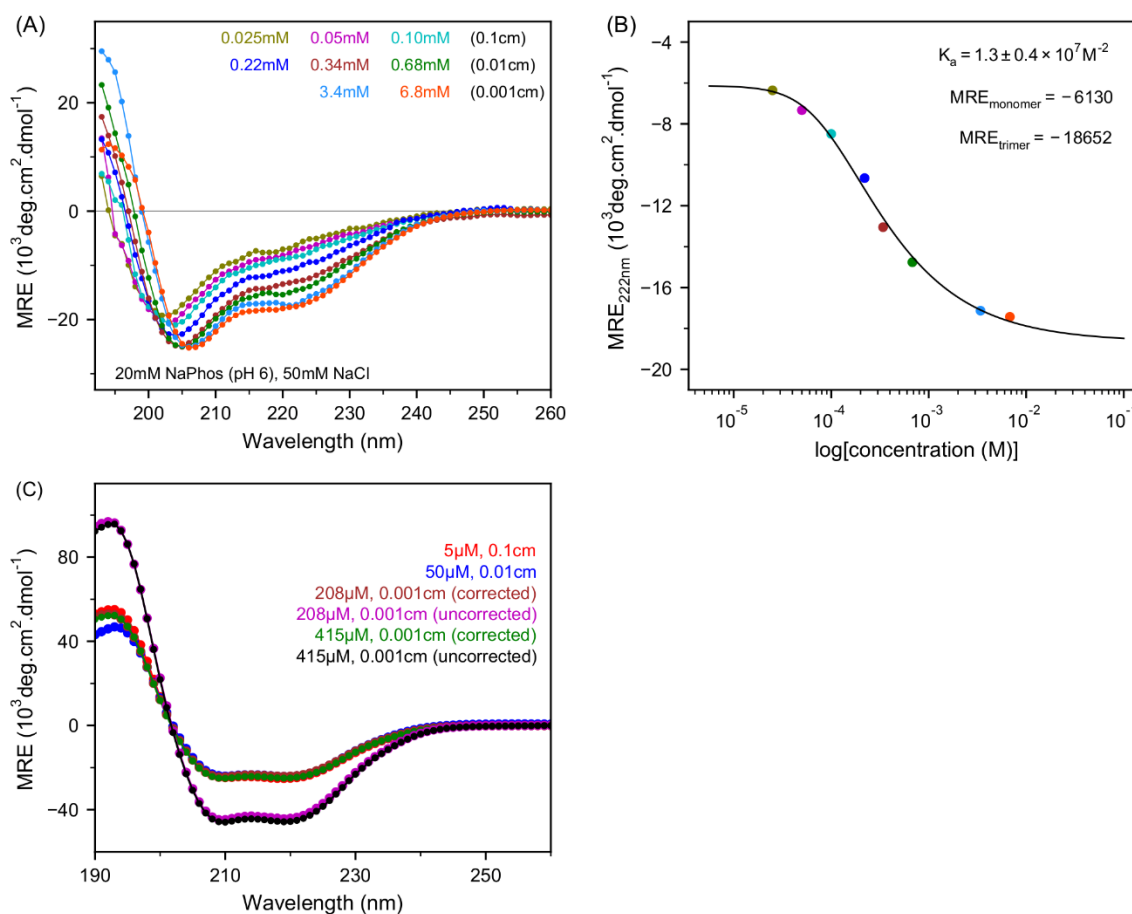
**Figure S1.** 1D <sup>1</sup>H NMR spectra of MPER. Downfield region of <sup>1</sup>H NMR spectra of MPER at 14.1 mM (red), 3 mM (green), 1.1 mM (blue) and 0.1 mM (black). Data were collected in 50 mM MES buffer (pH 6) at 35 °C. Ac- denotes N-terminal acetylation of the N-terminal Gly residue. Residue numbering corresponds to full length gp41 and residues K<sup>1</sup> to K<sup>5</sup> belong to poly-Lys tag.

Figure S2



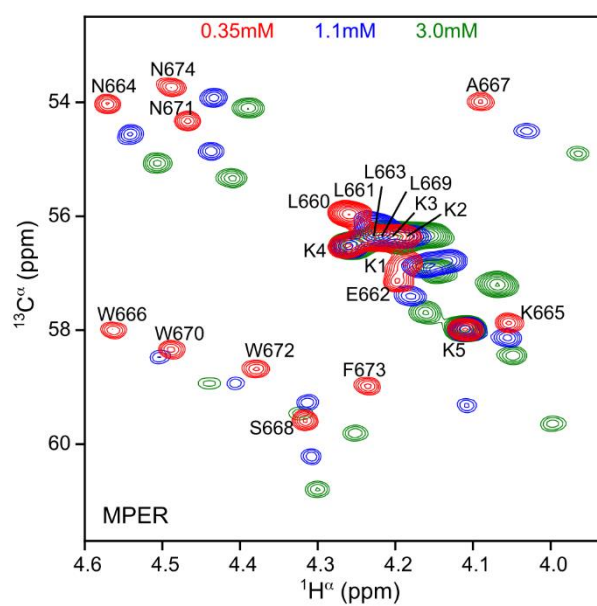
**Figure S2.** Effect of  $D_2O$  on MPER trimerization. (A) Overlay of  $^1H$ - $^{13}C$  HSQC excerpts recorded on samples containing 0.1 mM (black), 1.1 mM (blue) and 2.5 mM (red) MPER. (B) Methyl  $^1H$  chemical shifts for L663 and L669 at seven MPER concentrations (10  $\mu$ M to 14.5 mM). Global fitting of the data to a monomer-trimer equilibrium (solid black line) resulted in  $K_a = 3.8 \pm 0.1 \times 10^5 M^{-2}$  ( $\chi^2 = 7.9 \times 10^{-5} ppm^2$ ). Dashed lines represent the optimized fit to a monomer-dimer equilibrium with  $K_a = 3.0 \times 10^{-2} M^{-1}$  ( $\chi^2 = 2.0 \times 10^{-3} ppm^2$ ). Spectra were acquired at 35  $^\circ C$  in 50 mM MES buffer (pH 6), 99.8%  $D_2O$ .

Figure S3



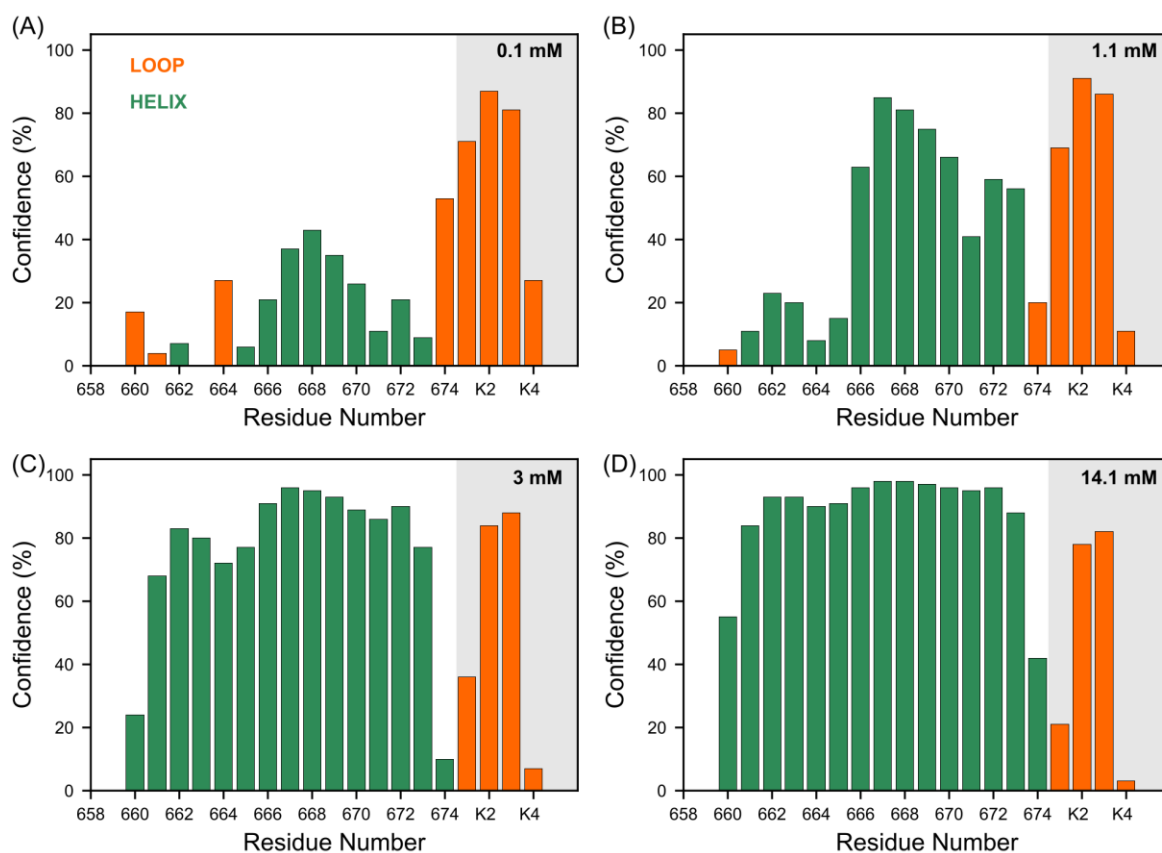
**Figure S3.** MPER structural transition as monitored by CD spectroscopy. (A) Far-UV CD spectra of MPER as a function of concentration. (B) Plot of mean residue ellipticity at 222 nm versus concentration. The colour scheme denoting various concentrations is the same for panels A and B. Fit of the data to a monomer-trimer model yields  $K_a \approx 1.3 \times 10^7 \text{ M}^{-2}$  and MRE values (at 222 nm) of -6130 (~18.6% helix) and -18652 (~56.5% helix) in the limits of monomer and trimer, respectively. These estimates are based on a  $[\theta]_{222}$  value of  $-33000 \text{ deg cm}^2 \text{ dmol}^{-1}$  for a perfect  $\alpha$ -helix.<sup>[5]</sup> (C) Control CD spectra of a single chain 6-helix bundle (6HB) for verifying pathlengths of cuvettes used. Data collected on a 0.001 cm path length cuvette resulted in traces (magenta and black, uncorrected), which when scaled by a factor of 0.55 (brown and green, corrected) matched with the signals obtained at 5  $\mu$ M and 50  $\mu$ M concentration using 0.1 cm and 0.01 cm cells, respectively. This observation is consistent with prior controlled studies performed on small pathlength cuvettes, also reporting a significant correction factor.<sup>[6-7]</sup> Thus, a scaling factor of (0.55) was applied to all data acquired for MPER in 0.001-cm cells to match with data acquired using 0.01 and 0.1 cm cells. Spectra were acquired at 25 °C in 20 mM sodium phosphate buffer (pH 6) and 50 mM NaCl.

Figure S4



**Figure S4.** MPER  $^{13}\text{C}\alpha$  chemical shifts. Overlay of  $^1\text{H}$ - $^{13}\text{C}$  HSQC excerpts acquired on samples containing 0.35 mM (red), 1.1 mM (blue) and 3 mM (red) MPER. Assignments are marked for the 0.35 mM sample. Spectra were acquired at 35 °C in 50 mM MES buffer (pH 6).

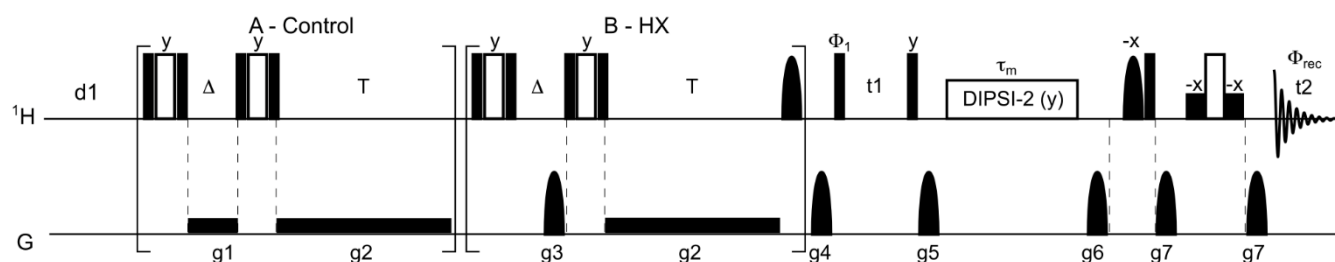
Figure S5



**Figure S5.** Secondary structure propensity in MPER at various sample concentrations (A) 0.1 mM, (B) 1.1 mM, (C) 3 mM and (D) 14.1 mM. The percentage of confidence in estimating the secondary structure was obtained from  $^1\text{H}^{\text{N}}$ ,  $^{15}\text{N}$ ,  $^{13}\text{C}^{\alpha}$  and  $^1\text{H}^{\alpha}$  chemical shifts using the TALOS-N program.<sup>[8]</sup> Green and orange bars represent helix and loop secondary structure, respectively. Chemical shifts were recorded in 50 mM MES (pH 6) at 35 °C. The C-terminal poly-Lys residues are shown on a grey background.

## SUPPORTING INFORMATION

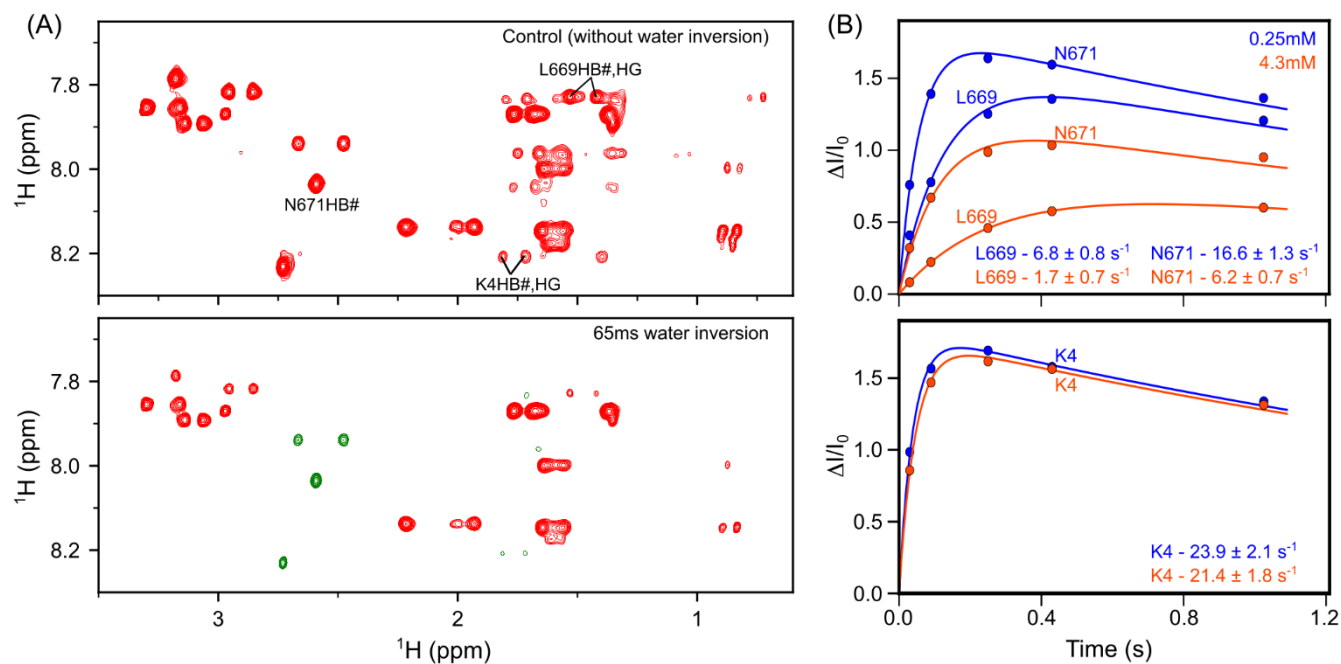
Figure S6



**Figure S6.** Pulse diagram of the WEX-III TOCSY experiment, used to measure HX rates. Filled and open  $^1\text{H}$  pulses represent  $90^\circ$  and  $180^\circ$  pulses, respectively. All RF phases are  $x$  unless otherwise noted. The  $^1\text{H}$  carrier frequency is set to the water resonance. The delay  $\Delta$  is set to 30 ms and serves to return the  $\text{H}_2\text{O}$  magnetization to the  $+z$  axis by radiation damping when no gradient is applied (Block B). Exchange rates are measured by incorporating Block-B (and removing Block-A) and by varying the delay 'T', over a range of 5-1000 ms, while the control experiment was performed in the absence of Block-B, and setting T to 1 ms. A TOCSY mixing time ( $\tau_m$ ) of 80 ms was used by implementing DIPSII-2 scheme.<sup>[9]</sup> Shaped  $^1\text{H}$  pulses correspond to the water-selective, center lobe of a  $\text{sinc}(x)$  function with a 2-ms pulse duration. The final  $180^\circ$  pulse is flanked by two 1.2-ms, water-selective rectangular pulses to aid water-suppression.<sup>[10]</sup> Quadrature in the indirect dimension was obtained using States-TPPI. All the pulsed field gradients are sine-bell shaped, except  $g_1$  and  $g_2$  (weak rectangular). Gradient strengths (and durations) are set to  $g_1= 3 \text{ G/cm}$   $g_2= 0.8 \text{ G/cm}$ ,  $g_3= 30.6 \text{ G/cm}$  (2 ms),  $g_4= 20.4 \text{ G/cm}$  (0.73 ms),  $g_5= 13.8 \text{ G/cm}$  (1.5 ms),  $g_6= 12.6 \text{ G/cm}$  (1 ms), and  $g_7= 25.8 \text{ G/cm}$  (0.37 ms). Phase cycling for  $\Phi_1=(x, -x)$  and  $\Phi_{\text{rec}} = (x, -x, -x, x)$ .

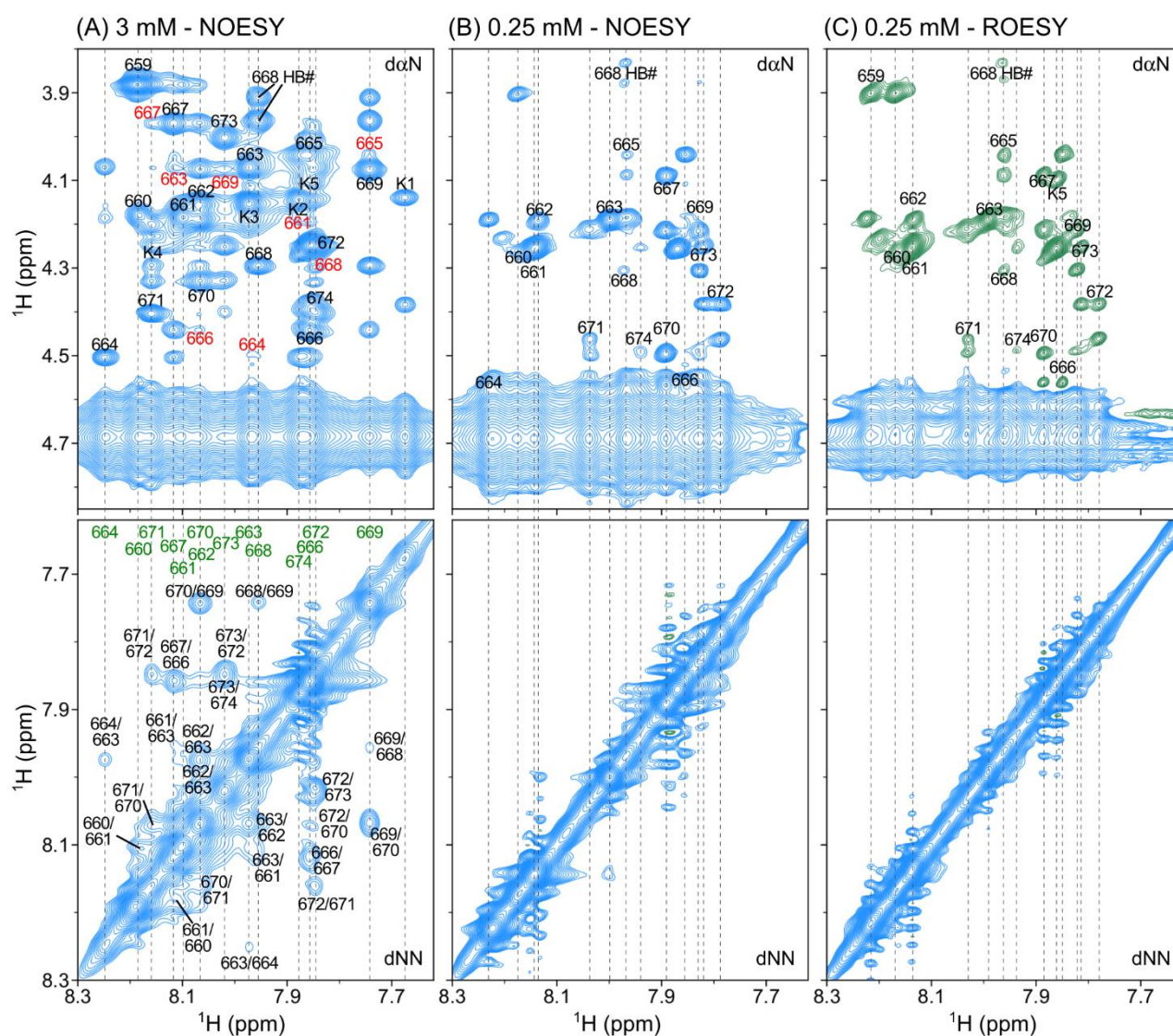
## SUPPORTING INFORMATION

Figure S7



**Figure S7.** Measurement of backbone amide HX rates of MPER. (A) Excerpt from  $\text{H}^{\text{all}}\text{-H}^{\text{N}}$  region of a 2D-TOCSY spectrum recorded at 800 MHz, without (top panel) and with (bottom panel) selective water inversion preceding the first  $90^\circ$  pulse by 65 ms, recorded on a sample containing 0.25 mM MPER in 10 mM imidazole buffer (pH 6.2) and  $35^\circ\text{C}$ , recorded with the pulse scheme of Figure S6. Red and green cross peaks represent positive and negative intensities, respectively. (B) Plots for the ratio of signal intensity as a function of water inversion mixing times, where  $I_0$  and  $I_{\text{inv}}$  are the intensities of cross-peaks in the absence and presence of water inversion ( $\Delta I = I_0 - I_{\text{inv}}$ ). Fitting to the data was performed as described elsewhere.<sup>[4]</sup> The top panel shows residues N671 and L669 from the structured region of MPER which exhibit quite different HX rates at 0.25 mM (blue) and 4.3 mM (orange). The bottom panel shows HX rate analysis for K678 from the disordered C-terminal host sequence which does not show significant HX attenuation at elevated peptide concentration.

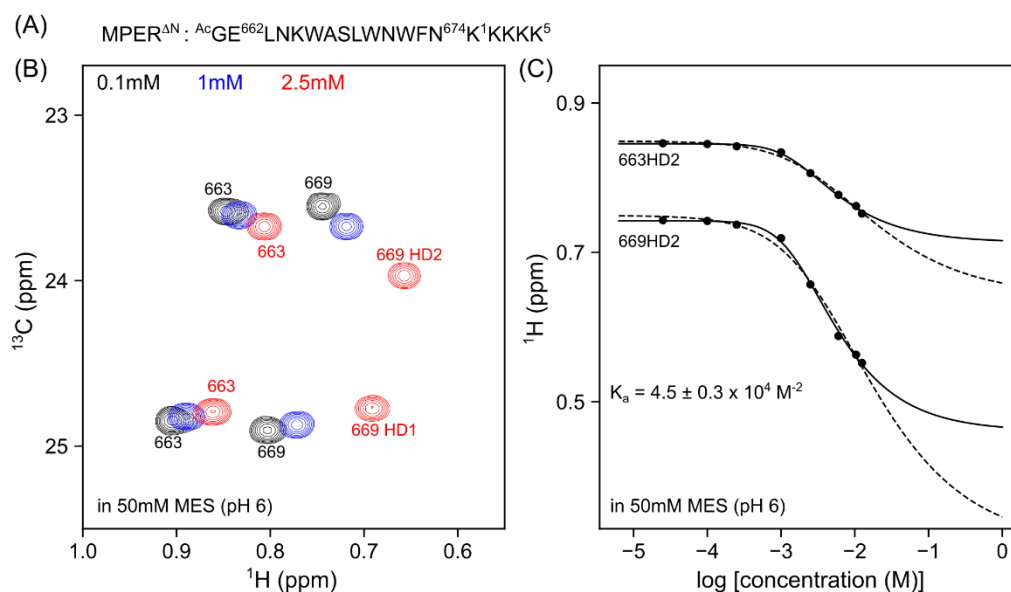
Figure S8



**Figure S8.** Small regions taken from 800 MHz 2D  $^1\text{H}$ - $^1\text{H}$  NOESY/ROESY spectra recorded on samples containing (A) 3 mM and (B, C) 0.25 mM MPER. Top panels correspond to the  $\text{H}^{\text{N}}$ - $\text{H}^{\text{N}}$  region, where the labels in black represent the  $\text{H}^{\text{N}}$  chemical shifts of the  $i^{\text{th}}$  residue, and  $d_{\alpha\text{N}}(i, i+4)$  NOEs are labeled in red. Bottom panels correspond to the  $\text{H}^{\text{N}}$ - $\text{H}^1$  region. Residue numbers for the diagonal peaks are shown in green, and NOE cross-peaks are shown in black. NOESY spectra were collected using a 200-ms mixing time, and the ROESY spectrum was collected using a 100-ms mixing time with a spin-lock field of 7kHz. All three spectra were collected at 35  $^{\circ}\text{C}$ , in 10 mM imidazole buffer, pH 6.2.

## SUPPORTING INFORMATION

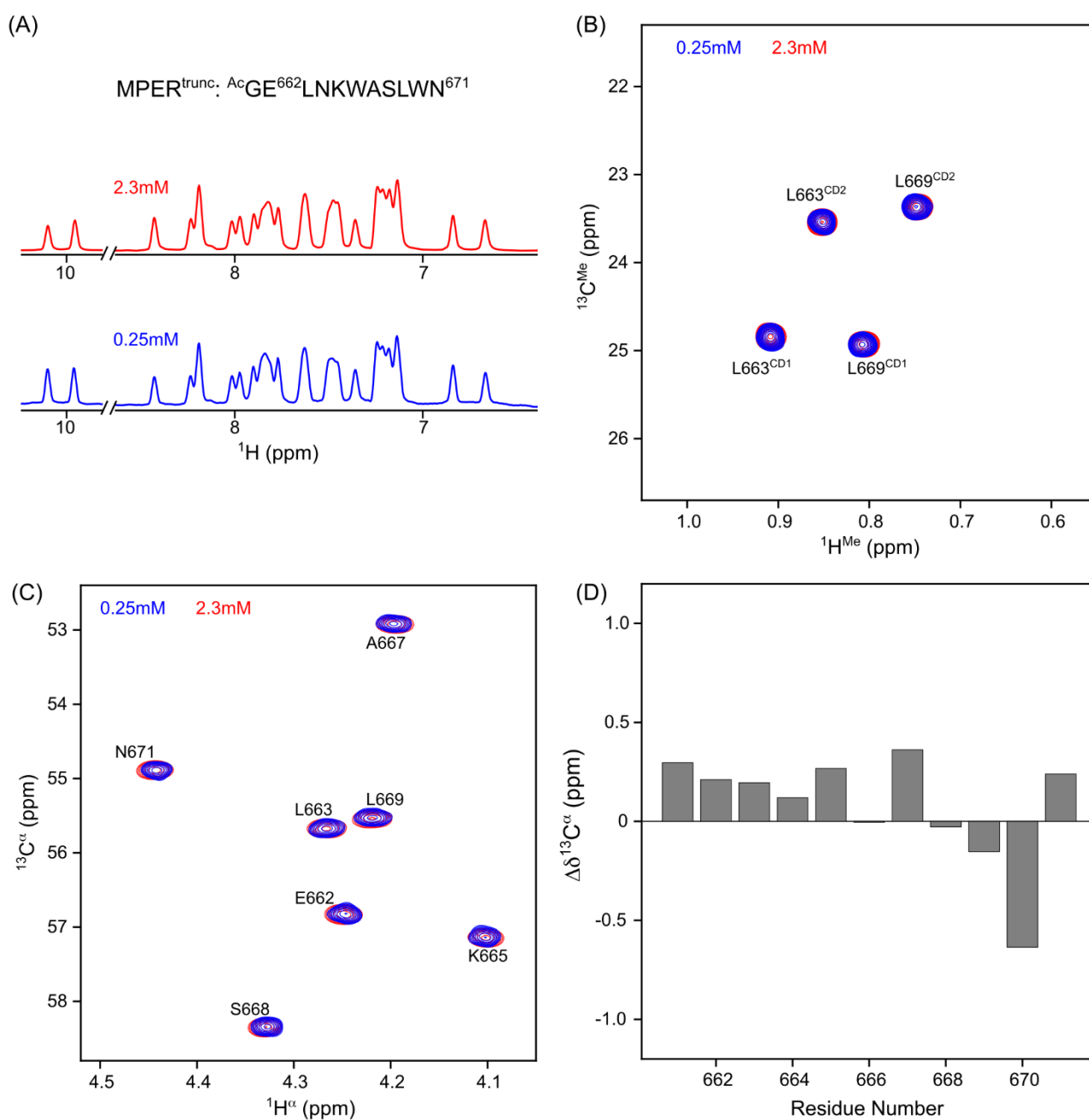
Figure S9



**Figure S9.** Effect of the deletion of two N-terminal leucines on MPER self-association. (A) Amino acid sequence of MPER $\Delta$ N. (B) Overlay of  $^1\text{H}$ - $^{13}\text{C}$  HSQC excerpts acquired on samples containing 0.1 mM (black), 1 mM (blue) and 2.5 mM (red) MPER $\Delta$ N. (C) Plot showing methyl  $^1\text{H}$  chemical shifts for L663 and L669 at eight different sample concentrations (25  $\mu\text{M}$  to 12.5 mM) of MPER $\Delta$ N. Global fitting of the data to monomer-trimer equilibrium (solid black line) resulted in  $K_a$  of  $4.5 \times 10^4 \text{ M}^{-2}$  ( $\chi^2$  for the fit =  $3 \times 10^{-4} \text{ ppm}^2$ ). Dashed lines represent the optimized fit to a monomer-dimer equilibrium with  $K_a$  of  $1.6 \times 10^{-2} \text{ M}^{-1}$  ( $\chi^2$  for the fit =  $1.5 \times 10^{-3} \text{ ppm}^2$ ). Spectra were acquired at 35  $^\circ\text{C}$  in 50 mM MES buffer (pH 6).

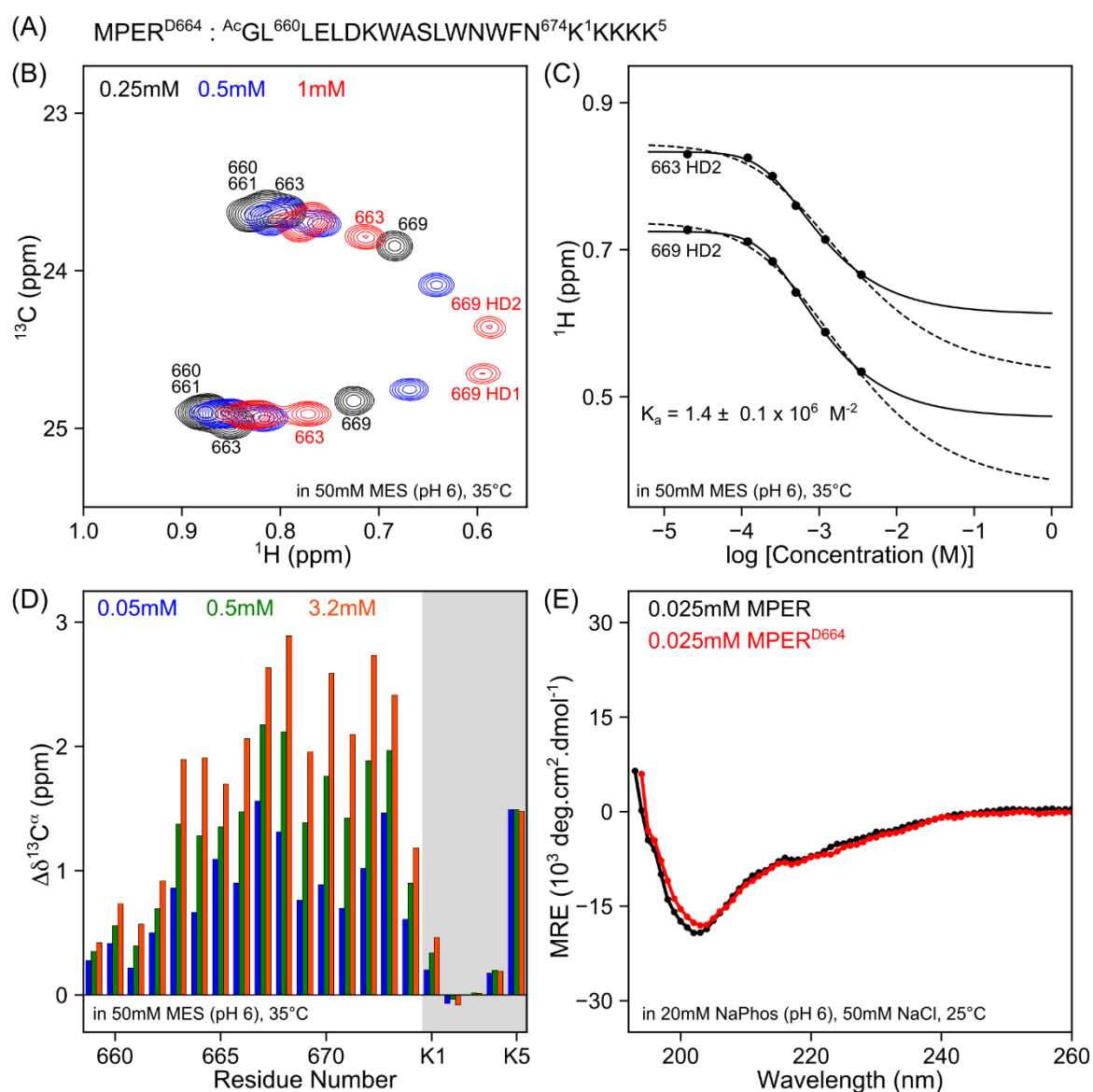
## SUPPORTING INFORMATION

Figure S10



**Figure S10.** Lack of self-association in MPER<sup>trunc</sup>. (A) <sup>1</sup>H NMR spectra at 2.3 mM (red) and 0.25 mM (blue). (B) Methyl and (C) <sup>13</sup>C<sup>α</sup> region from <sup>1</sup>H-<sup>13</sup>C HSQC spectra of MPER<sup>trunc</sup>. (D) The small magnitudes of deviations of <sup>13</sup>C<sup>α</sup> chemical shifts from the neighbor-corrected random coil values point to a dynamically disordered, random-coil-like conformational ensemble of MPER<sup>trunc</sup>. Spectra were acquired at 35 °C in 50 mM MES buffer (pH 6).

Figure S11



**Figure S11.** MPER<sup>D664</sup> monomer-trimer equilibrium. (A) Amino acid sequence of MPER<sup>D664</sup>. (B) Overlay of <sup>1</sup>H-<sup>13</sup>C HSQC excerpts recorded on samples containing 0.25 mM (black), 0.5 mM (blue) and 1 mM (red) MPER<sup>D664</sup>. (C) Methyl <sup>1</sup>H chemical shifts for L663 and L669 at six different sample concentrations (20 μM to 3.2 mM) of MPER<sup>D664</sup>. Global fitting of the data to a monomer-trimer equilibrium (solid black line) resulted in  $K_a = 1.4 \times 10^6 \text{ M}^{-2}$  ( $\chi^2 6.2 \times 10^{-5} \text{ ppm}^2$ ). Dashed lines represent the optimized fit to a monomer-dimer equilibrium with  $K_a = 4.5 \times 10^2 \text{ M}^{-1}$  ( $\chi^2 8.7 \times 10^{-4} \text{ ppm}^2$ ). (D) Residue-specific secondary  $\Delta\delta^{13}\text{C}^\alpha$  chemical shifts of MPER<sup>D664</sup> (0.05 mM – blue; 0.5 mM – green; 3.2 mM – orange). NMR data were acquired at 35 °C in 50 mM MES buffer (pH 6). The C-terminal poly-Lys tag residues are shown on a grey background. (E) Overlay of the far-UV CD spectra of MPER<sup>D664</sup> (red) with MPER (black), signifying very similar secondary structures at 25 μM. CD spectra were acquired in 20 mM sodium phosphate buffer (pH 6) and 50 mM NaCl at 25 °C.

## SUPPORTING INFORMATION

**Table S1.** Hydrogen exchange (HX) rates of MPER at 4.3 mM and 0.25 mM concentrations in 10 mM Imidazole buffer (pH 6.2) and 35 °C.

Residue	HX <sub>4.3mM</sub> (s <sup>-1</sup> )	HX <sub>0.25mM</sub> (s <sup>-1</sup> )
G659	4.0 (±0.7)	3.4 (±0.6)
L660	8.3 (±0.7)	6.9 (±0.7)
L661	3.7 (±0.8)	3.2 (±0.8)
E662	3.3 (±0.9)	3.4 (±0.8)
L663	2.5 (±0.7)	2.7 (±0.7)
N664	10.5 (±0.8)	11.4 (±1.0)
K665	8.9 (±0.9)	15.4 (±1.3)
W666	1.8 (±0.7)	4.1 (±0.8)
A667	NA	5.7 (±0.8)
S668	10.4 (±1.0)	15.2 (±1.3)
L669	1.7 (±0.7)	6.8 (±0.8)
W670	NA	2.7 (±0.7)
N671	6.2 (±0.7)	16.6 (±1.3)
W672	2.0 (±0.7)	7.0 (±0.8)
F673	1.7 (±0.7)	5.2 (±0.9)
N674	9.3 (±0.9)	22.8 (±1.9)
K1	10.7 (±0.9)	23.9 (±2.0)
K2	NA	NA
K3	16.6 (±1.3)	19.5 (±1.7)
K4	21.4 (±1.8)	23.9 (±2.1)

## Author Contributions

SCC carried out all NMR measurements, analyzed the data and drafted the original manuscript; JML carried out CD experiments and edited the manuscript; AB directed the study and edited the manuscript.

## References

- [1] F. Delaglio, S. Grzesiek, G. W. Vuister, G. Zhu, J. Pfeifer, A. Bax, *J. Biomol. NMR* **1995**, *6*, 277-293.
- [2] J. J. Helmus, C. P. Jaroniec, *J. Biomol. NMR* **2013**, *55*, 355-367.
- [3] J. M. Louis, A. Aniana, K. Lohith, J. M. Sayer, J. Roche, C. A. Bewley, G. M. Clore, *PLoS One* **2014**, *9*.
- [4] N. C. Fitzkee, D. A. Torchia, A. Bax, *Protein Sci.* **2011**, *20*, 500-512.
- [5] E. O'Shea, R. Rutkowski, P. Kim, *Science* **1989**, *243*, 538-542.
- [6] S. M. Kelly, T. J. Jess, N. C. Price, *BBA-Proteins Proteomics* **2005**, *1751*, 119-139.
- [7] A. J. Miles, F. Wien, J. G. Lees, B. A. Wallace, *Spectroscopy* **2005**, *19*, 263649.
- [8] Y. Shen, A. Bax, *J. Biomol. NMR* **2013**, *56*, 227-241.
- [9] A. J. Shaka, C. J. Lee, A. Pines, *J. Magn. Reson.* **1988**, *77*, 274-293.
- [10] M. Piotto, V. Saudek, V. Sklenar, *J. Biomol. NMR* **1992**, *2*, 661-665.